International Journal of Biological Macromolecules 82 (2016) 798–805

Contents lists available at ScienceDirect

International Journal of Biological Macromolecules

journal homepage: www.elsevier.com/locate/ijbiomac

Rapana thomasiana hemocyanin modified with ionic liquids with enhanced anti breast cancer activity

Maya Guncheva[a,*], Krasimira Paunova[a], Paula Ossowicz[b,c], Zbigniew Rozwadowski[c], Ewa Janus[b], Krassimira Idakieva[a], Svetla Todinova[d], Yuliana Raynova[a], Veselina Uzunova[d], Sonia Apostolova[d], Rumiana Tzoneva[d], Denitsa Yancheva[a]

[a] Institute of Organic Chemistry with Centre of Phytochemistry, Bulgarian Academy of Sciences, Acad. G. Bonchev Str. bl. 9, 1113 Sofia, Bulgaria
[b] Institute of Organic Chemical Technology, West Pomeranian University of Technology Szczecin, Pulaski Str. 10, 70-322 Szczecin, Poland
[c] Department of Inorganic and Analytical Chemistry, West Pomeranian University of Technology Szczecin, Piastow 42, 71-065, Szczecin, Poland
[d] Institute of Biophysics and Biomedical Engineering, Bulgarian Academy of Sciences, Acad. G. Bonchev Str., bl. 21, 1113 Sofia, Bulgaria

ARTICLE INFO

Article history:
Received 17 August 2015
Received in revised form 9 October 2015
Accepted 11 October 2015
Available online 23 October 2015

ABSTRACT

This is the first study on the surface modification of a hemocyanin from marine snail *Rapana thomasiana* (RtH) with series of imidazolium-based amino acid ionic liquids [emim][AA]. We monitored the induced by [emim][AA] conformational changes in RtH molecule and evaluated the effect of these ionic liquids (ILs) on the protein thermal stability. The cytotoxicity of all obtained RtH-[emim][AA] complexes was assessed toward breast cancer cells (MCF-7) and murine fibroblasts (3T3).

As a whole, even small amounts of the tested ILs altered the secondary structure of RtH. The thermal denaturation of RtH in presence of [emim][AA] displayed multi-component transitions, which were shifted toward lower temperatures in comparison to those estimated for the native RtH. The profiles of the RtH-IL calorimetric curves show a clear dependence on the structure of the added salts. In addition, all RtH-[emim][AA] complexes exhibited an enhanced antiprofilerative activity of toward MCF-7 cells in comparison to that of the native RtH. The best results are observed for RtH-[emim][Leu], RtH-[emim][Trp] or RtH-[emim][Ile], which applied in concentration of 700 μg/mL inhibited the MCF-7 cell viability (for 24 h) by 66, 63 and 53%, respectively. In addition, these IL-RtH complexes were less cytotoxic to 3T3 cells, i.e. they exhibited some cell specificity.

1. Introduction

Ionic liquids (ILs) are molten salts comprising of an organic cation and an organic or an inorganic anion. They are considered as environmentally friendly media due to their low melting points (<100 °C), low vapor pressures, non flammability, thermal and chemical stabilities, controlled miscibility with organic solvents and water, etc. [1,2]. It is noteworthy to be mentioned that, being highly polar yet noncoordinating solvents, ILs are able to dissolve wide range of inorganic and organic materials, which makes them suitable media for synthetic organic and biocatalytic reactions and extraction solvents for biopolymers, secondary plant metabolites and/or synthetic products in separation technologies [3–6]. By altering the structure of either the cation or the anion of ILs, a directed "tuning" of their physicochemical properties can be achieved, which makes ILs applicable in many other fields beside synthesis and catalysis. For example, some ILs are industrially applied as electrolytes for batteries, engineering fluids (hydraulic, cleaning and cooling liquids), liquid supports for storage of gases, etc. [6]. In recent years, an increasing attention has been paid to the biomedical application of ILs. For example, there are reports on the synthesis of pharmaceutically active ILs with improved solubility, bioavailability and pharmacokinetics and increased anti-bacterial, anti-inflammatory and anti-allergic properties in comparison to their conventional counterparts [7,8]. In addition, it has been shown that numerous pure ILs are potent antimicrobial and anti-cancer agents [9,10]. In last decade, with the fast development of biotechnological drugs (mono-and bifunctional antibodies, fusion and plasma derived proteins, growth factors, vaccines, etc.), a special attention has been paid to the methods for their stabilization. Ionic liquids have potential to be a good alternative to conventional protein stabilizers (polyols, carbohydrates, surfactants, salts, etc.) [11]. For example, Kumar and Venkatesu have observed that some short-chain alkyl imidazolium-based and

* Corresponding author. Tel.: +359 29606160; fax: +359 28700225.
E-mail address: maiag@orgchm.bas.bg (M. Guncheva).

http://dx.doi.org/10.1016/j.ijbiomac.2015.10.031
0141-8130/

ammonium-based ILs stabilize insulin [12,13]. High-yield extraction of proteins, antibodies and enzymes and at the same time their preserved native or active conformation in cholinium-based ionic liquid buffers have also been reported [14,15]. The effect of 1-ethyl-3-methyl-imidazolium-based ILs as refolding additives and suppressors of protein aggregation have been estimated for cardioactive peptides, lysozyme, recombinant plasminogen activators, antibody fragments, etc. [16,17]. In addition, ILs come to help in studies of protein unfolding or misfolding and amyloid fibril formation processes associated with many neurodegenerative and autoimmune diseases [18]. Furthermore, it is well known that the protein function is tightly related to its structure. Up to date only the interactions between small number of ILs and relatively small proteins have been investigated. There are scarce data on the influence of ILs on the conformational stability and the biological activity of large proteins.

The aim of this study is to investigate the influence of a series of biocompatible ILs, containing 1-ethyl-3-methyl-imidazolium cation and amino acid anion [emim][AA], on the conformation and anti-cancer activity of a hemocyanin isolated from the hemolymph of marine snails *Rapana thomasiana* [RtH]. RtH is a complex type-3 copper protein (9MDa) comprising of twenty subunits organized in a hollow cylinder. Each subunit contains of eight covalently bound functional units, each of them bearing a pair of Cu(II) ions capable of reversible binding of a dioxygen molecule, i.e. active centre [19,20]. The biological function of hemocyanins (Hcs) is to transport oxygen throughout the bodies of some invertebrate animals. Recently, Hcs have been of considerable medicinal interest in cancer immunotherapy due to their high immunogenicity [21,22]. In addition, Tchorbanov et al. have achieved enhanced antigen immunogenicity for the epitope of influence A virus hemagglutinin bound to RtH or its subunits and they have suggested that Hcs can be successfully used in many immunization protocols as adjuvants or protein carriers [23]. Gesheva et al. have demonstrated the potential of RtH as cancer preventive vaccine, which was tested "in vivo" experiments with murine model of colon carcinoma [24].

Arancibia et al. have made a correlation between structural stability and immunogenicity of the oxidized by sodium periodate *Concholepas concholepas* hemocyanin [25]. To best of our knowledge there are no other studies on the dependence of the secondary structure of Hcs on their anti-cancer activities. Moreover, this is the first study on the interactions between imidazolium-based ILs and Hcs, particularly RtH. The selection of the series of the ILs to be tested with Hcs is based on the plenty of literature data on the beneficial effect of ILs, containing short alkyl chain imidazolium cation and various anions on activity, selectivity and stability of many proteases and oxidoreductases, as well as promoters of oxidative folding of cysteine-rich proteins, in some cases better solvents to proteins [17,18,26].

We assessed the effect of the [emim][AA] on the conformation, thermal stability and antiproliferative activity against MCF-7 and 3T3 cells of RtH. All results are compared with those of non-treated native RtH.

2. Materials and methods

2.1. Materials

L-methionine, glycine, L-valine, L-leucine, L-threonine, L-isoleucine, L-tryptophan (>99%) were purchased from Carl Roth. 1-Ethyl-3-methylimidazolium chloride ([emim][Cl] (≥97 wt.%), DMSO-d_6 and Dowex Monosphere 550 A UPW (OH form) resin were provided by Sigma-Aldrich. Absolute ethanol (99.8%) was purchased from Chempur.

Murine embryotic fibroblast (3T3) and human breast cancer (MCF-7) cell lines were purchased from American Type Culture Collection (ATCC).

Thiazolyl Blue Tetrazolium Bromide (MTT) (98%) was purchased from Sigma. RPMI-1640, DMEM high glucose media, L-glutamine and sodium bicarbonate were purchased from PAN-Biotech GmbH, Aidenbach, Germany.

2.2. Synthesis and characterization of the 1-ethyl-3methylimidazolium amino acids

1-Ethyl-3-methylimidazolium L-methionate ([emim][Met]), 1-ethyl-3-methylimidazolium glycinate ([emim][Gly], 1-ethyl-3-methylimidazolium L-valinate ([emim][Val]), 1-ethyl-3-methylimidazolium L-leucinate ([emim][Leu]), 1-ethyl-3-methylimidazolium L-threoninate ([emim][Thr]), 1-ethyl-3-methylimidazolium L-isoleucinate ([emim][Ile]), 1-ethyl-3-methylimidazolium L-tryptophanate ([emim][Trp]), and 1-ethyl-3-methylimidazolium L-histidinate ([emim][His]) were synthesized via two-step procedure. Initially, the chloride anion in imidazolium chloride was exchanged to hydroxide anion on the ion exchange resin. Then, so obtained 1-ethyl-3-methylimidazolium hydroxide was reacted with the corresponding amino acid (Scheme 1). The detailed synthetic procedure and characteristics of the organic salts are given in the electronic supporting file.

2.3. Isolation of RtH and formation of its complexes with the ILs

The protein used in this study was isolated from the hemolymph of marine snails *Rapana thomasiana* as previously described [27]. Using the absorption coefficient A_{278} = 1.36 mg^{-1} mL cm^{-1} (20 °C), the concentration of the RtH stock solution was determined to be 38 mg/mL.

To obtain RtH-[emim][AA] complexes, RtH (1.52 mg/mL) was incubated with various amounts of [emim][AA] (from 0.001 M to 0.1 M) at 25 °C for 0, 20, 40, 60 and 1440 min.

Native gel electrophoresis in 7.5% polyacrylamide gel (native-PAGE) was applied as analytical method for initial characterization of the protein stability in presence of [emim][AA]. Samples from native RtH and RtH-IL complexes were prepared in sodium phosphate buffer (pH 7.2, 5 mM). The electrophoresis was performed by the method of Laemmli [28] but under non-denaturing conditions and in the absence of SDS. The protein bands were visualized by silver staining.

2.4. UV–vis spectroscopy

The absorption spectra for RtH and its complexes with [emim][AA] were recorded on Evolution™ 300 UV–Vis Spectrophotometer (Thermo Electron Corporation) equipped with a Peltier temperature control accessory with the highest resolution (1 nm) using matched 1 cm path length quartz cuvettes. The reference cuvette was filled with sodium phosphate buffer (pH 7.2, 5 mM) and contained the same concentration of the corresponding IL. Repeat scanning was performed for each sample in order to monitor the absorbance changes over time.

2.5. Fourier transformed infrared spectroscopy

Infrared spectra of the RtH (30.4 mg/mL) dissolved in sodium phosphate buffer (pH 7.2, 5 mM) or in 0.2 M aqueous solution of [emim][AA] (in the same buffer) were recorded on Bruker Tensor 27 spectrometer, equipped with deuterated triglycine sulphate detector (DTGS). Each sample was deposited onto a diamond crystal (ATR element) and a 128 scan interferogram was collected in a single beam mode, with 1 cm^{-1} resolution from 4000 to 600 cm^{-1}.

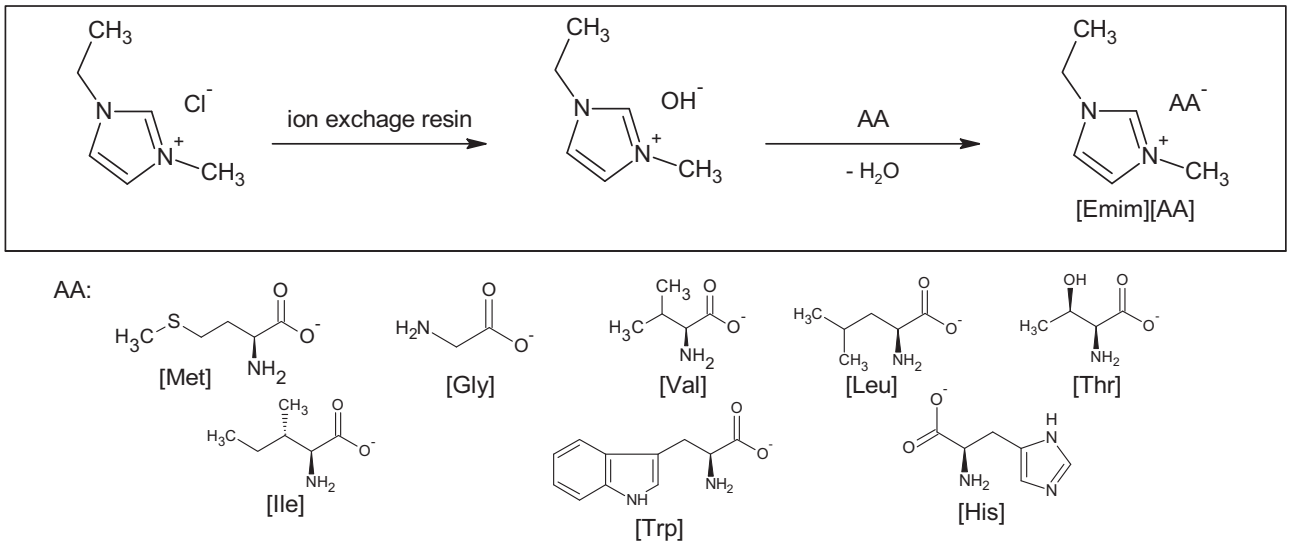

Scheme 1. Synthesis path and structures of 1-ethyl-3-methylimidazolium-based amino acid ionic liquids [emim][AA].

Reference spectra containing the corresponding IL in the same concentration were recorded. A baseline correction was performed in the amide I region (1600–1700 cm^{-1}) assuming a linear baseline. In order to enhance the component peaks contributing to Amide I band the spectra were treated by Fourier-self deconvolution using Opus software version 5.5. Second derivative spectra were obtained using the Savitzky-Golay algorithm based on 21 smoothing points. The line shape was Lorentzian with a half-bandwidth of 14 cm^{-1} and an enhancement factor of 2.9 was used. The assignment of the Amide I band positions to secondary structure was done according to the literature data [29].

2.6. Differential scanning calorimetry (DSC)

The changes in the phase transitions of RtH in presence of [emim][AA] were performed on DASM 4 (Privalov, BioPribor)-built-in highly sensitive calorimeter with cell volumes of 0.5 mL, a sensitivity >0.017 mJ K^{-1} and a noise level below 0.05 μW under the previously described experimental conditions [19].

2.7. Cytotoxicity test

The RtH-[emiml][AA] complexes were obtained by incubation of 80 μL RtH (38 mg/mL stock) with 20 μL of 1 M aqueous solution of the corresponding [emim][AA] at room temperature for 60 min. Their effect on cell viability of two cell lines, 3T3 murine fibroblasts (non cancerous cells) and breast cancer cell line MCF-7 was estimated with colorimetric test using a tetrazolium dye (MTT assay) [30]. The detailed procedure is given in the electronic supplementary file.

2.8. Statistical analysis

All statistical calculations were carried out with Graph Pad Prism software (Graph Pad Software Inc., San Diego, USA). Data were analyzed by one-way ANOVA followed by Tukey–Kramer post-hoc test. The values were considered to be significantly different if the p value was <0.01.

3. Results and discussion

3.1. Effect of [emim][AA] on RtH structure

3.1.1. Native-PAGE experiment/analysis

In native-PAGE the electrophoretic mobility of proteins depends on their net charge, size and shape of the native structure. Thus native gels are sensitive to any process that alters either the charge or the conformation of a protein.

At first, we subjected samples from native RtH and RtH-IL complexes in sodium phosphate buffer (pH 7.2, 5 mM) to the native-PAGE in order to check the effect of the ILs on the size and charge of the protein. As can be seen in Fig. 1, no changes are observed in the native-PAGE profiles of RtH-[emim][AA]-complexes in comparison to that of the non-treated RtH. The incubation of RtH (1.52 mg/mL) with the tested [emim][AA] did not cause a chemical degradation of the protein or a dramatic change of its overall structure or an aggregation.

In comparison, Kumar and Venkatesu has reported for up to 95% decrease in the hydrodynamic radii of insulin in presence of small

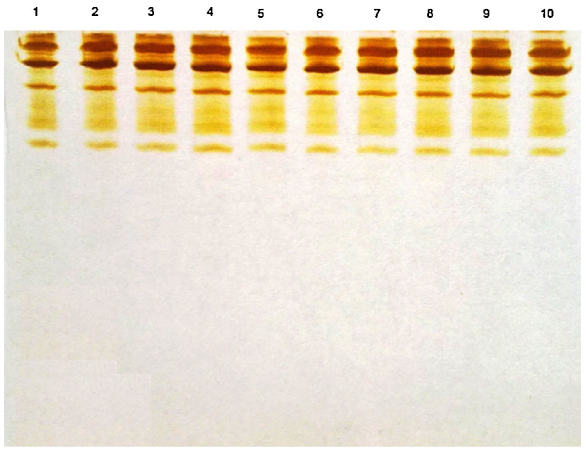

Fig. 1. Native polyacrylamide gel electrophoresis on 7.5% running gel. Lane 1 (and lane 10), native RtH; lane 2, RtH-[emim][Gly]; lane 3, RtH-[emim][Val]; lane 4, RtH-[emim][Leu], lane 5, RtH-[emim][Ile]; lane 6, RtH-[emim][Met]; lane 7, RtH-[emim][Trp]; lane 8, RtH-[emim][His]; lane 9, RtH-[emim][Thr].

amounts of 1-butyl-3-methylimidazolium ILs, which they ascribed to either stabilization of insulin in a monomeric form or cleavage of its interchain disulfide bonds, which resulted in presence of smaller segments [12].

3.1.2. UV–vis spectroscopy

The absorption spectrum of the native RtH in sodium phosphate buffer (pH 7.2, 5 mM) is characterized with two bands: a strong band with maximum at 280 nm, which is due to the tryptophyl and the tyrosyl residues of the protein; and a second band, due to the copper(II)–peroxide complex at the active sites, which has moderate intensity and is located at 345 nm. According to the literature data, the fully oxygenated RtH exhibits *A*345/*A*280 absorbance ratio of 0.25 [31]. In all experiments, we kept constant the amount of RtH (1.52 mg/mL, ca 0.17 μM) and varied the concentration of the ILs in the cuvette. In presence of [emim][AA], we observed a decrease in the intensity of the two characteristic absorption bands in a concentration-dependent manner. The spectra of RtH in presence of various concentrations of [emim][Ile] are given in Fig. 2A as an example.

Added at the lowest tested concentration (0.001 M), the valinate, the methionate and the threoninate analogues have no effect on RtH structure. At the same concentration, the strongest effect on RtH was produced by [emim][Gly] and [emim][Leu] resulting in decrease in the absorbance intensity of the two bands by 10%. The conformational changes in RtH, induced by that small amount of ILs occur quickly and no further changes in the absorption spectra were recorded with time. The time-series of UV–vis absorbance spectra of RtH in presence of 0.001 M [emim][Ile] are shown in Fig. 2B as an illustration.

The higher concentrations of ILs (0.01 M) have the same time-independent hypochromic effect on the two bands. For all ILs, except for [emim][Met], the decrease in the intensity of the bands at 280 and 345 nm in RtH spectra varies between 15 and 20% depending on the structure of the anion. For the methionate derivative, the effect is much stronger and the reduction of intensity of the two bands is 30% (Fig. S1). Interestingly, the effect of [emim][Met] added in much higher concentration (0.1 M) is weaker (Fig. S1). For the rest of [emim][AA], except for the isoleucinate salt, we did not register changes in RtH absorption spectra, when the concentration was raised up to 0.1 M (Fig. S2).

The quenching of the absorption bands at 280 nm in presence of [emim][AA] is probably due to conformational changes in the hemocyanin molecule, which lead to disturbance of the microenvironment of tryptophyl and tyrosyl residues. Changes in the catalytic active conformation of the active sites of the protein cause a decrease of the intensity of characteristic band at 345 nm. In the absorption spectra of most of the RtH-[emim][AA]complexes this band is slightly affected, thus we assume that the oxygen-binding properties of hemocyanin active sites are preserved.

The ratio of RtH (1.52 mg/mL, 0.17 μM) to [emim][AA] (0.01 M) was kept constant in the subsequent experiments.

3.1.3. FTIR spectroscopy

We monitored the changes in the Amide I region in the FTIR spectra of RtH in presence of [emim][AA] in order to assess their impact on the secondary structure of RtH. For that purpose, the spectra of the native and the IL-treated RtH were collected, smoothed and baseline corrected (Fig. S3 A-J). Then, they were deconvoluted in the 1700–1600 cm^{-1} region and a curve fitting procedure was applied for quantitative estimation of the area of each secondary structural element. In the spectra of the all modified hemocyanins, we observed peaks located at the following frequency intervals: 1660–1650 cm^{-1}, 1638–1610 cm^{-1}, 1680–1660 cm^{-1}, 1648–1638 cm^{-1} and 1692–1680 cm^{-1} corresponding to α-helical structures, β-sheets, β-turns, random coils and anti-parallel β-sheets, respectively. The calculated percentages of each secondary structural element, which are found in the spectra of the native and the modified RtH are given in Table 1. A close similarity was found between the structures of the native and the [emim][Gly]-treated RtH. However, the glycinate salt seems to promote RtH aggregation at the tested protein to IL ratio. RtH underwent dramatic conformational changes in presence of the other tested here IL. Except for RtH-[emim][Gly] and RtH-[emim][Trp], the additional bands, in the region 1600–1610 cm^{-1}, assigned to side-chain vibrations of amino acid residues, are observed in the spectra of all IL-treated RtH. We assume that due to a conformational change induced by the last mentioned ILs some of the buried inside the RtH side-chain amino acid residues appeared on the protein surface (Table 2).

Distinct dissimilarities between the spectrum of RtH in 0.01 M [emim][Leu] and those in 0.01 M [emim][Ile] are found, although the only differences between the two ILs was in the position of the anion side-chain branching. In [emim][Ile] we observed a complete loss of the band attributed to the unordered structures or random coils and considerable increase in the bands for β-sheets and β-turns. In contrast, RtH-[emim][Leu] spectrum was characterized with a slight increase in α-helical and β-turn structures in comparison to that of the native RtH. We assume that in this case more compact structure is realized. Arfmann et al. have observed that peptide polymers containing leucine preferably occupy α-helical conformation, while those containing isoleucine—β-conformation [32]. Thus, we assume that the leucinate and the isoleucinate salts, although not chemically bonded to the protein, participated in strong hydrophobic interaction with some of RtH hydrophobic amino acid residues and possibly were nuclei for local formation of these secondary structures.

Fall in both α-helical and β-sheet structures in favor of unordered structures (random coils and β-turns) was observed in the spectrum of RtH in 0.01 M [emim][Met] suggesting that the protein was partially unfolded and occupied conformation that is distant from the native one.

Surprisingly, despite of the differences in their structure and properties (H-bonding, hydrophobic interactions), [emim][Trp] and [emim][Thr] have similar effect on RtH conformation. In presence of these two ILs we observed increase in α-helices and β-sheets, i.e. more ordered RtH conformation was stabilized. In addition, tryptophanate salt seems to suppress effectively the protein aggregation. On the other hand, histidinate salt seemed to affect only α-helical and coil structures and preserved β-structures.

It is difficult for us to speculate on specific interactions between [emim][AA] and RtH because of the complex structure of hemocyanins. For instance, only for the anion of histidinate salt are possible five types of interactions (cation π-interactions, π–π stacking interactions, hydrogen-π interactions, coordinate bond interactions, and hydrogen bond interactions) with many different amino acid residues of the protein.

We can summarize that the secondary structure of RtH depends strongly on the structure of [emim][AA] and even small variations in the anion resulted in completely different protein conformation, which differed also from that of the native RtH.

3.2. Effect of [emim][AA] on RtH thermal stability

Thermal stability of RtH and its complexes with [emim][AA] was assessed by high-sensitivity differential scanning calorimetry. The denaturation of RtH proceeded as endothermic process over the temperature range 53–94 °C in IL-free system, but it was shifted by 10 °C toward the lower temperatures for all RtH-IL-treated samples. The thermal denaturation of RtH dissolved in phosphate buffer (pH 7.2, 5 mM) with or without [emim][AA] added display multi-component transitions. This is probably due

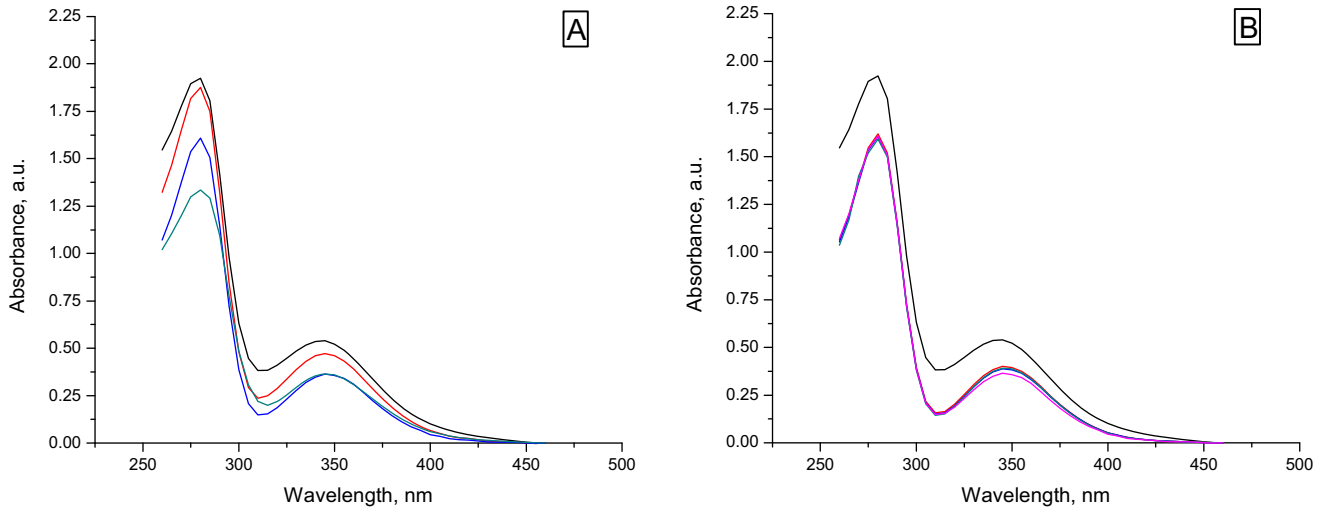

Fig. 2. (A) UV–vis absorbance of RtH (1.52 mg/mL), dissolved in sodium phosphate buffer (pH 7.2, 5 mM) containing different amount of [emim][Ile]: IL-free (black), 0.001 M (red), 0.01 M (blue), 0.1 M (green) recorded after 24 h incubation. (B) Time evolved UV–vis absorption spectra of RtH, dissolved in sodium phosphate buffer (pH 7.2, 5 mM) containing 0.01 M [emim][Ile]: 0 min (red), 20 min (blue), 40 min (green) and 24 h (cyan). For comparison is given the spectrum of RtH in sodium phosphate buffer without IL (black). (For interpretation of the references to color in this figure legend, the reader is referred to the web version of the article.)

Table 1
Quantitative estimation of the secondary structural elements of native hemocyanin from *Rapana thomasiana* and its complexes with 1-ethyl-3-methylimidazolium-based amino acid salts calculated from their curve fitted FTIR spectra.

Sample	α-Helix (%)	β-Sheet (%)	Random coils (%)	β-Turn (%)	H-bonded aggregates (%)	Amino acid side chains (%)
RtH	15.16	33.62	23.86	13.39	13.97	NA
RtH-[emim][Gly]	15.80	26.84	18.87	15.10	23.38	NA
RtH-[emim][Val]	9.65	31.66	14.42	18.75	18.47	7.06
RtH-[emim][Leu]	16.48	31.87	13.85	16.23	12.00	9.57
RtH-[emim][Ile]	14.31	45.80	NA	23.30	12.76	3.82
RtH-[emim][Met]	10.65	24.11	27.70	18.53	11.48	7.53
RtH-[emim][Trp]	22.10	41.24	23.94	10.84	1.88	NA
RtH-[emim][Thr]	26.67	46.70	NA	12.42	6.55	1.99
RtH-[emim][His]	11.81	35.92	12.57	18.02	16.3	5.88

[a]Prior to measurements, RtH (30.4 mg/mL) was incubated with sodium phosphate buffer (pH 7.2, 5 mM) containing 0.2 M of the coresponding [emim][AA] for 60 min at 25 °C.

to interactions of the sodium phosphate buffer and the added organic salts with the stabilizing Ca^{2+} and Mg^{2+} ions that present in RtH, which on other hand results in "repacking" of the molecule upon unfolding. The observed DSC profile is in agreement with earlier findings of Idakieva et al. for thermal denaturation of native RtH in various buffer solutions [19]. The obtained complex thermograms for all samples are shown in Fig. 3, along with their deconvolution patterns. The profiles of the RtH-IL calorimetric curves show a clear dependence on the structure of the added salts. For all RtH-[emim][AA] complexes no thermal effect was observed in the second subsequent scan, which was an indication for the irreversibility of the thermal denaturation. The results are consistent with those reported in the literature for native RtH and other Hcs [19]. For all IL-treated RtH we estimated the parameters ($T_{m,i}$, $\Delta H_{cal,i}$) of each component peak obtained after the deconvolution analysis of the heat capacity functions (Table 1). As can be seen, the thermal stability of RtH was seriously affected in presence of [emim][AA]. Depending on the IL structure, all transition peaks were shifted toward lower temperatures (up to 13.6 °C). In presence of [emim][Gly] and [emim][Val] we observed additional low temperature shoulders centered at 49.7 and 49.4 °C. We noticed essential differences in total heat uptake estimated for each RtH-IL-complex. The value of ΔH_{total} was the highest for the non-treated RtH and in terms of decreasing ΔH_{total} values the resulting anion series of the tested salts reads: $[Gly^-] > [Leu^-] > [Ile^-] > [Met^-] > [His^-] > [Val^-] \approx [Thr^-] > [Trp^-]$. Analyzing these results we can find a good correlation between the effect of [emim][AA] on RtH secondary structure and the resulted

Table 2
Summary of DCS characteristics of multi-component transition for the thermal unfolding process of RtH in presence of [emim][AA], obtained from the deconvoluted spectra.

Sample	T_{m1} (°C)	ΔH_{1cal} (kJ/mol)	T_{m2} (°C)	ΔH_{2cal} (kJ/mol)	T_{m3} (°C)	ΔH_{3cal} (kJ/mol)	T_{m4} (°C)	ΔH_{4cal} (kJ/mol)	T_{m5} (°C)	ΔH_{5cal} (kJ/mol)	ΔH_{tot} (kJ/mol)
RtH	72.9	32688.0	74.5	64386.0	80.6	26183.0	87.8	20222.0	–	–	141571
RtH + [emim][Gly]	49.7	3401.0	60.1	64723.6	67.1	20555.5	72.2	31966.7	77.0	14363.6	135215
RtH + [emim][Val]	49.4	1519.0	59.4	47615.1	66.8	21173.9	72.3	30029.3	77.0	11688.4	112307
RtH + [emiml][Leu]	–	–	61.9	70066.2	67.8	7789.8	74.8	55586.3	–	–	131790
RtH + [emiml][Ile]	60.1	49747.7	67.0	20791.5	71.5	7949.4	74.9	47956.5	–	–	124382
RtH + emim][Met]	62.5	49034.7	69.6	36654.2	73.6	3025.1	77.6	29156.3	–	–	117285
RtH + [emim][Trp]	59.9	50742.7	66.7	14152.3	71.7	26137.0	78.3	17046.2	–	–	107611
RtH + [emim][His]	61.4	40125.6	68.6	33106.4	72.9	4433.9	77.1	37445.3	–	–	114711
RtH + [emiml][Thr]	63.8	64900.0	69.8	20074.1	74.1	6217.9	78.0	21343.7	–	–	112026

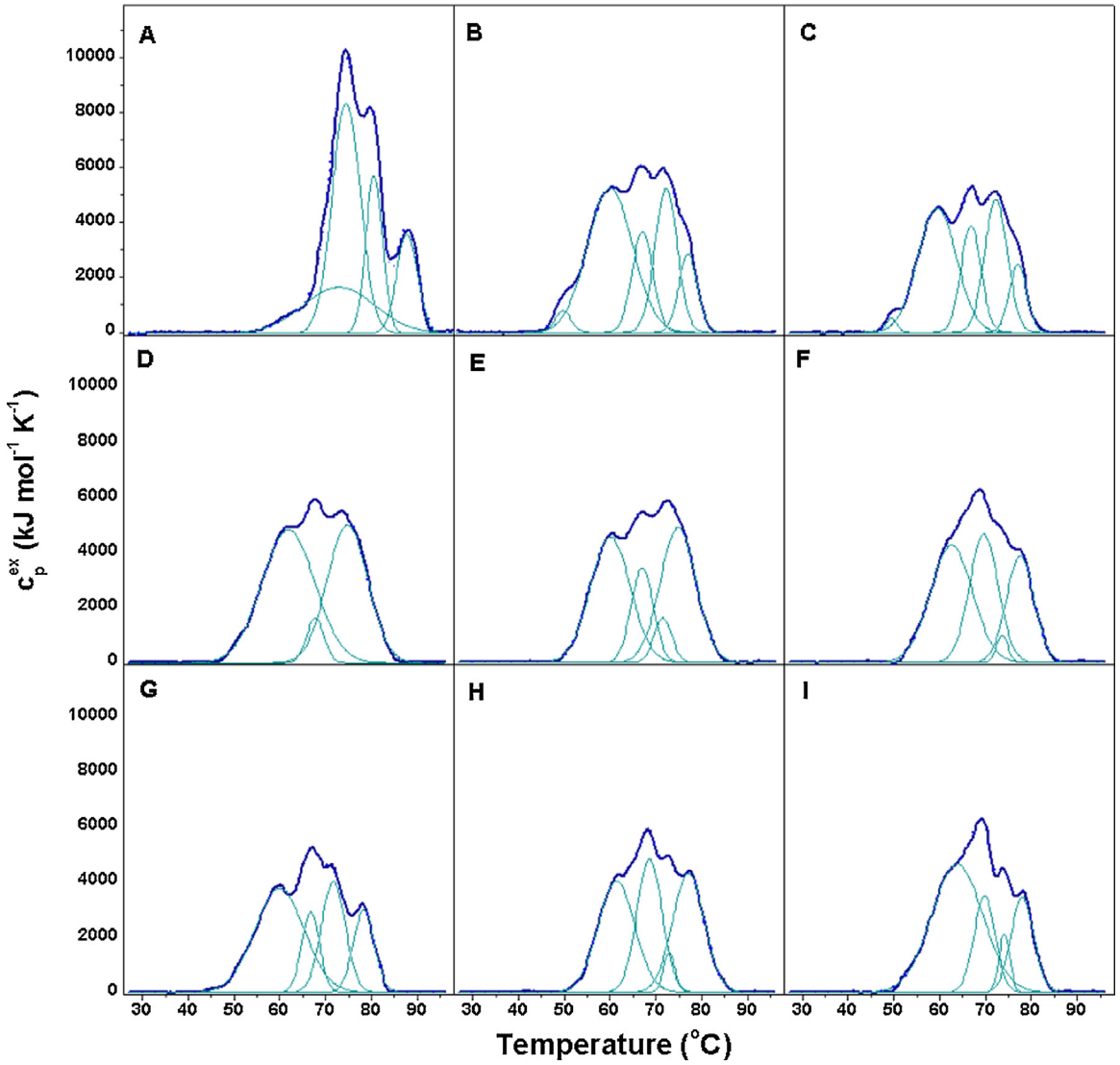

Fig. 3. Thermal denaturation profiles of native RtH in sodium phosphate buffer (pH 7.2, 5 mM) (A); RtH-[emim][Gly] (B); RtH-[emim][Val] (C); RtH-[emim][Leu] (D); RtH-[emim][Ile] (E); RtH-[emim][Met] (F); RtH-[emim][Trp] (G); RtH-[emim][His] (H); RtH-[emim][Thr] (I). The blue lines show the experimental curves and the green lines represent component peaks, obtained by deconvolution analysis of the excess heat capacity function. Heating rate was 1 °C/min. (For interpretation of the references to color in this figure legend, the reader is referred to the web version of the article.)

thermal stability of the corresponding sample. The conformational analysis showed that the glycinate and the leucinate complexes of RtH are the closest to the native RtH fold, which explains their highest thermal stability within the RtH-[emim][AA] series. In contrast, an increase in both α-helical content and β-sheets structures were observed for RtH in presence of tryptophanate and threoninate salts, i.e. highly ordered structures of RtH were realized, which were the most non-native and the least heat stable. Decrease in α-helices in favor of either β- or unordered structures were observed for RtH in presence of the imidazolium salts containing isoleucyl, methionyl, histidyl or valyl anions. These ILs had moderate effect on the RtH thermal stability within the series of the tested compounds.

3.3. Cytotoxicity of [emim][AA] and RtH-[emim][AA]-complexes on fibroblasts and breast cancer MCF-7 cells

To assess what is the effect of the IL-induced structural changes in RtH on its biological activity we applied MTT assay as proxy for cell viability and compared the cytotoxic effects of all RtH-[emim][AA] complexes on cultured human breast cancer cells (MCF-7) and fibroblasts (3T3 cells, non-cancerous cells). The IL-modified protein was tested in a concentration range from 100 to 700 μg/mL and results were compared with those obtained with native RtH. Control experiments with samples containing only [emim] salts in concentrations of 0.67 mM and 4.7 mM, corresponding to the lowest and the highest amount of ILs introduced into the system with the RtH-complexes.

To the best of our knowledge there are no available literature data on the anti-cancer activity of imidazolium-based amino acids or their complexes with therapeutic proteins. We found that at the tested concentrations most of the studied here [emim][AA] produced weak (10–15%) to moderate (15–20%) antiproliferative effects toward MCF-7 and 3T3 cells (Fig. 4A, Fig. 5A). The cell viabilities were much lower but of approximately the same magnitude for the two cell lines in presence of 4.7 mM [emim][Val] or [emim][Trp] and did not exceed 65 and 50%, respectively. It is noticeable that isoleucinate salt exhibited good cell specificity. Indeed, the viabilities of the MCF-7 and the 3T3 cell lines after incubation with 4.7 mM [emim][Ile] were determined to be 44.8 ± 4.3% and 77.8 ± 2.3%, respectively. The effect produced by [emim][AA] on MCF-7 cell viability is comparable to that reported by Kumar et al. for

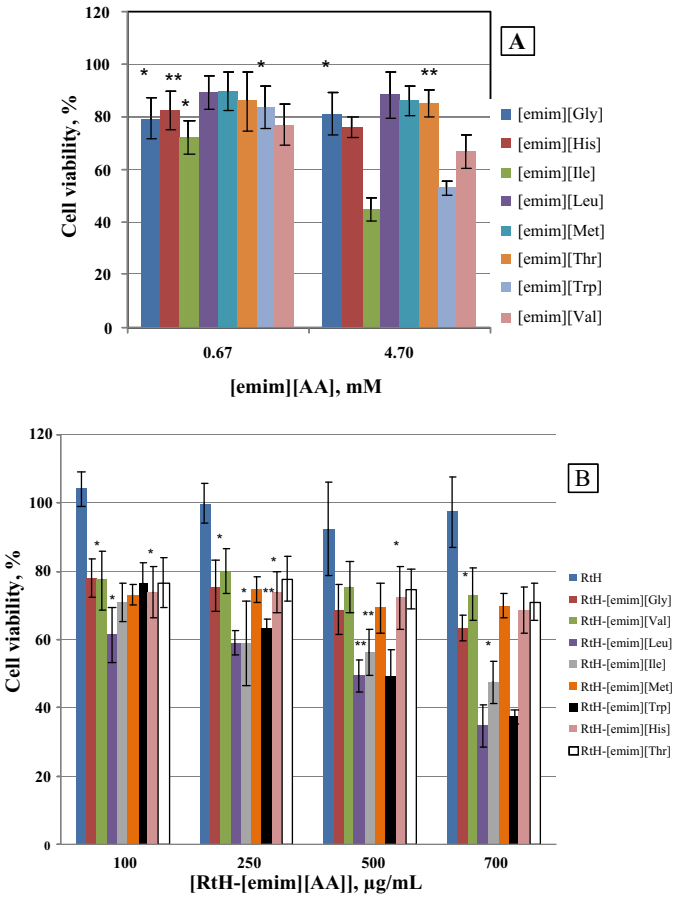

Fig. 4. Cell viability of MCF-7 after 24 h of incubation in presence of [emim][AA] (A) and their complexes with RtH (B). Data are means Environ ± SD of eigth replicates. The statistic was performed by ANOVA test. $^{*}p < 0.01$, $^{**}p < 0.001$.

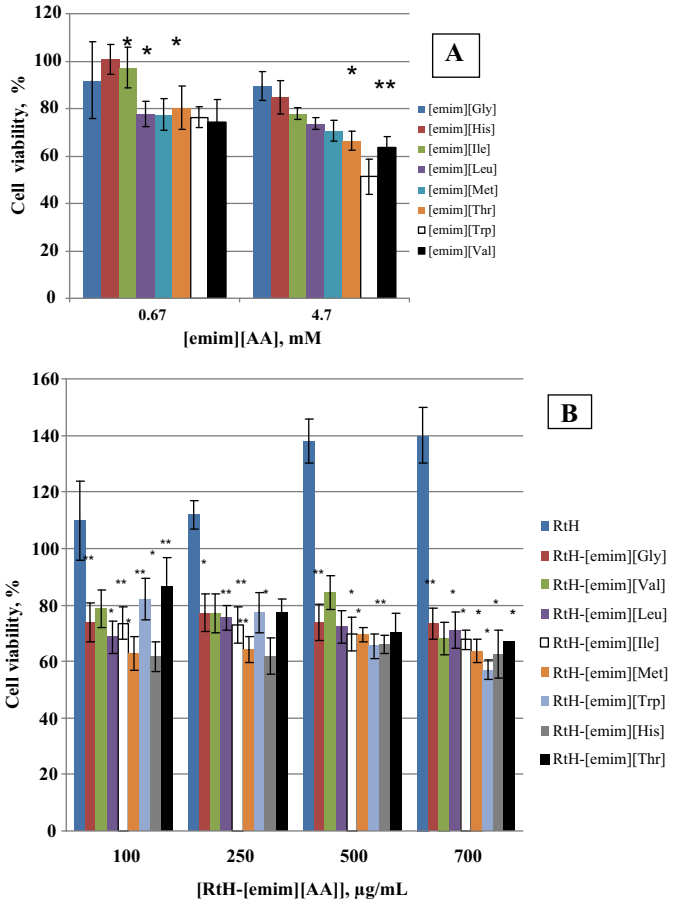

Fig. 5. Cell viability of 3T3 cells after 24 h of incubation in presence of [emim][AA] (A) and their complexes with RtH (B). Data are means ± SD of eigth replicates. The statistical analysis was performed by ANOVA test. $^{*}p < 0.01$, $^{**}p < 0.001$.

1-alkyl-3methylimidazolium bis[trifluoromethylsulfonyl]imide who estimated that tested toward the same cell line these compounds have IC_{50} ranging from 0.64 to 6.2 mM and their cytotoxic effect was strongly dependent on the chain length of the alkyl substituent at the cation [33].

The respective data on the effect of the native and IL-modified RtH on MCF-7 and 3T3 cell viabilities are shown in Fig. 4B and Fig. 5B. As can be seen, the native RtH stimulated the growth of fibroblasts in concentration-dependent manner. In contrast, at the same tested doses RtH has no effect on the MCF-7 viability. The highest MCF-7 inhibition was observed after treatment of the cells with leucinate, isoleucinate and thriptophanate RtH-complexes (Fig. 4B) and the observed cytotoxic effect strongly depended on the RtH-IL concentration. The viabilities of MCF-7 after a 24-h incubation with 700 μg/mL of RtH-[emim][Leu] was determined to be only 34.7 ± 6.1%, and with 700 μg/mL of RtH-[emim][Trp] or RtH-[emim][Ile] 37.3 ± 2.0% and 47.4 ± 6.1%, respectively. Similar concentration-dependent trend but about two fold weaker cytotoxic effect was estimated for these three IL-RtH complexes tested on fibroblasts. The more effective interactions of RtH-[emim][Leu], RtH-[emim][Ile] or RtH-[emim][Trp] with the more acidic membrane of the cancer cells is a possible explanation to their stronger antiproliferative effect on MCF-7 cells in comparison to that of the referent non-cancerous cells.

Interestingly, RtH-[emim][Val] and RtH-[emim][Met] appeared to be more cytotoxic to 3T3 cells than toward the breast cancer cells and the observed decreased cell viability was not dose-related and was stronger for the non cancerous cells.

On the other hand, RtH complexes with the glycinate, the valinate and the threoninate salts did not demonstrate any selectivity in cell growth inhibition of the two tested cell lines and their activities were slightly dependent of the applied concentration.

In summary, the enhanced antiproliferative activity on breast cancer cells of RtH-[emim][AA]-complexes in comparison to that of the non-modified RtH is probably due to their more appropriate conformation, which ensure stronger interaction with the cell membranes. The cytotoxic effect on MCF-7 cells obtained with RtH complexes with leucinate, isoleucinate and tryptophanate salts is comparable with that reported for Hc from Keyhole limpet (KLH)—39 ± 9.1% growth inhibition of MCF-7 after 72 h-incubation with 100 μg KLH [34]. Although the immunostimulating and anticancer properties of various hemocyanins have been intensively studied no other data on the effect of Hcs on MCF-7 cells, except those found for KHL, are available.

4. Conclusion

We found that even small variations in the anion structure of the imidazolium-based amino acid ILs induce significant changes in RtH secondary structure. Due to the altered structure, the IL modified-RtH is characterized with decreased thermal stability and enhanced cytotoxicity on MCF-7 cells. Some of RtH-[emim][AA] complexes exhibit good cell specificity, i.e. inhibit more effectively breast cancer than non-cancerous cells. Thus, we think that the modification of RtH and other Hcs with various ILs is worth to be

thoroughly investigated, especially in respect to the anti-cancer potential of these proteins.

Appendix A. Supplementary data

Supplementary data associated with this article can be found, in the online version, at http://dx.doi.org/10.1016/j.ijbiomac.2015.10.031.

References

[1] T. Welton, Ionic liquids in catalysis, Coordin. Chem. Rev. 248 (2004) 2459–2477.
[2] Ph. Jessop, D. Jessop, D. Fu, Lam Phan, Solvatochromic parameters for solvents of interest in green chemistry, Green Chem. 14 (2012) 1245–1259.
[3] J. Hallett, T. Welton, Room-temperature ionic liquids: solvents for synthesis and catalysis. 2, Chem. Rev. 111 (2011) 3508–3576.
[4] F. van Rantwijk, R.A. Sheldon, Biocatalysis in ionic liquids, Chem. Rev. 107 (2007) 2757–2785.
[5] T. Fan, C. Chen, T. Fan, F. Liu, Q. Peng, Novel surface-active ionic liquids used as solubilizers forwater-insoluble pesticides, J. Hazard. Mater. 297 (2015) 340–346.
[6] H. Olivier-Bourbigou, L. Magna, D. Morvan, Ionic liquids and catalysis: recent progress from knowledge to applications, Appl. Catal. A-Gen. 373 (2010) 1–56.
[7] K. Bica, H. Rodrıguez, G. Gurau, O.A. Cojocaru, A. Riisager, R. Fehrmann, R.D. Rogers, Pharmaceutically active ionic liquids with solids handling, enhanced thermal stability, and fast release, Chem. Commun. 48 (2012) 5422–5424.
[8] J. Shamshina, P. Barber, R. Rogers, Ionic liquids in drug delivery, Expert Opin. Drug Deliv. 10 (2013) 1367–1381.
[9] K. Docherty, Ch. Kulpa, Toxicity and antimicrobial activity of imidazolium and pyridinium ionic liquids, Green Chem. 7 (2005) 185–189.
[10] R.A. Kumar, N. Papaïconomou, J.-M. Lee, J. Salminen, D. Clark, J.M. Prausnitz, In *vitro* cytotoxicities of ionic liquids: effect of cation rings, functional groups, and anions, Environ. Toxicol. 24 (2009) 388–395.
[11] L. Jorgensen, S. Hostrup, E. Moeller, H. Grohganz, Recent trends in stabilizing peptides and proteins in pharmaceutical formulations—considerations in the choice of excipients, Expert Opin. Drug Deliv. 6 (2009) 1219–1230.
[12] A. Kumar, P. Venkatesu, The stability of insulin in presence of short alkyl chain imidazolium based ionic liquids, RSC Adv. 4 (2014) 4487–4499.
[13] A. Kumar, P. Venkatesu, Prevention of insulin self-aggregation by protic ionic liquid, RSC Adv. 3 (2013) 362–367.
[14] M. Taha, M. Quentala, I. Correia, M.G. Freire, J.A.P. Coutinho, Extraction and stability of bovine serum albumin (BSA) using cholinium-based Good's buffers ionic liquids, Process Biochem. 50 (2015) 1158–1166.
[15] M. Taha, M.R. Almeida, F. Silva, P. Domingues, S. Ventura, J. Coutinho, M. Freire, Novel biocompatible and self-buffering ionic liquids for biopharmaceutical applications, Chem. Eur. J. 21 (2015) 4781–4788.
[16] R. Buchfink, A. Tischer, G. Patil, R. Rudolph, Ch. Lange, Ionic liquids as refolding additives: variation of the anion, J. Biotechnol. 150 (2010) 64–72.
[17] M. Böhm, A. Tietze, P. Heimer, M. Chen, D. Imhof, Ionic liquid as reaction media for oxidative folding and native chemical ligation of cysteine-containing peptides, J. Mol. Liq. 192 (2014) 67–70.
[18] H. Weingärtner, C. Cabrele, C. Herrmann, How ionic liquids can help to stabilize native proteins, Phys. Chem. Chem. Phys. 14 (2012) 415–426.
[19] K. Idakieva, K. Parvanova, Svetla Todinova, Differential scanning calorimetry of the irreversible denaturation of *Rapana thomasiana* (marine snail, Gastropod) hemocyanin, Biochim. Biophys. Acta 1748 (2005) 50–56.
[20] K. Idakieva, F. Meersman, C. Gielens, Reversible heat inactivation of copper sites precedes thermal unfolding of molluscan (*Rapana thomasiana*) hemocyanin, Biochim. Biophys. Acta 1824 (2012) 731–738.
[21] S. Baek, Y.-M. Kim, S.-B. Kim, C.-S. Kim, S.-W. Kwon, Y.M. Kim, H.S. Kim, H. Lee, Therapeutic DC vaccination with IL-2 as a consolidation therapy for ovarian cancer patients: a phase I/II trial, Cell. Mol. Immun. 12 (2015) 87–95.
[22] J. Gao, C. Bernatchez, P. Sharma, L.G. Radvanyi, P. Hwu, Advances in the development of cancer immunotherapies, Trends Immunol. 34 (2013) 90–98.
[23] A. Tchorbanov, K. Idakieva, N. Mihaylova, L. Doumanova, Modulation of the immune response using *Rapana thomasiana* hemocyanin, Int. Immunopharmacol. 8 (2008) 1033–1038.
[24] V. Gesheva, S. Chausheva, N. Mihaylova, I. Manoylov, L. Doumanova, K. Idakieva, A. Tchorbanov, Anti-cancer properties of gastropodan hemocyanins in murine model of colon carcinoma, BMC Immunol. 15 (2014) 34.
[25] S. Arancibia, M. Del Campo, E. Nova, F. Salazar, M.I. Becker, Enhanced structural stability of *Concholepas* hemocyanin increases its immunogenicity and maintains its non-specific immunostimulatory effects, Eur. J. Immunol. 42 (2012) 688–699.
[26] R. Patel, M. Kumari, A.B. Khan, Recent advances in the applications of ionic liquids in protein stability and activity: a review, Appl. Biochem. Biotech. 172 (2014) 3701–3720.
[27] K. Idakieva, S. Severov, I. Svendsen, N. Genov, S. Stoeva, M. Beltramini, G. Tognon, P. Di Muro, B. Salvato, Structural properties of *Rapana thomasiana* hemocyanin: isolation, characterization and N-terminal amino acid sequence of two different dissociation products, Comp. Biochem. Physiol. 106B (1993) 53–59.
[28] U.K. Laemmli, Nature, Cleavage of structural proteins during the assembly of the head of bacteriophage T4, Nature 227 (1970) 680–685.
[29] A. Barth, Infrared spectroscopy of proteins, BBA-Bioenergetics 1767 (2007) 1073–1101.
[30] T. Mosmann, Rapid colorimetric assay for cellular growth and survival: application to proliferation and cytotoxicity assays, J. Immunol. Meth. 65 (1983) 55–63.
[31] K. Idakieva, I. Chakarska, P. Ivanova, A. Tchorbanov, I. Dobrovolov, L. Doumanova, Purification of hemocyanin from marine gastropod *Rapana thomasiana* using ammonium sulfate precipitation method, Biotechnol. Biotec. Eq. 23 (2009) 1364–1367.
[32] H.-A. Arfmann, R. Labitzke, K. Wagner, Conformational properties of l-leucine, l-isoleucine, and l-norleucine side chains in l-lysine copolymers, Biopolymers 16 (1977) 1815–1826.
[33] R.A. Kumar, N. Papaïconomou, J.-M. Lee, J. Salminen, D.S. Clark, J.M. Prausnitz, In vitro cytotoxicities of ionic liquids: effect of cation rings, functional groups, and anions, Environ. Toxicol. 24 (2009) 388–395.
[34] D. Riggs, B. Jackson, L. Vona-Davis, D. McFadden, In vitro anticancer effects of a novel immunostimulant: keyhole limpet hemocyanin, J. Surg. Res. 108 (2002) 279–284.